Pakistan Veterinary Journal

ISSN: 0253-8318 (PRINT), 2074-7764 (ONLINE)
DOI: 10.29261/pakvetj/2026.027

RESEARCH ARTICLE

SGK1 Suppresses LPS-Induced Inflammatory Responses in Bovine Endometrium via miR-143/TAK1 Axis

Wen Feng[1], Han Zhou[2], Talha Umar[1], Nuoer Chen[1], Jinxin Zhang[1], Wenjing Liu[1], Liyang Li and Ganzhen Deng[1*]

[1]Department of Clinical Veterinary Medicine, College of Veterinary Medicine, Huazhong Agricultural University, Wuhan, People's Republic of China; [2]School of Physical Education and International Equestrianism, Wuhan Business University, Wuhan, 430070, People's Republic of China
*Corresponding author: dgz@mail.hzau.edu.cn

ARTICLE HISTORY (25-1080)

Received: November 08, 2025
Revised: December 09, 2025
Accepted: December 30, 2025
Published online: January 05, 2026

Key words:
Dairy Cow
Endometritis
SGK1
TAK1
miR-143

A B S T R A C T

Endometritis significantly reduces conception rates and milk production in the dairy cows. Serum and glucocorticoid inducible kinase 1 (SGK1) functions as an indispensable mediator of uterine receptivity dynamics during the estrus-mating transition period. It is also implicated in inflammatory processes; SGK1 signaling hubs in the Lipopolysaccharide (LPS) - Toll-like receptors 4 (TLR4) cascades require verification *via* endometrial epithelial cells specifically transgenic models. In this study, endometritis was first diagnosed by histopathological investigation, and confirmed by increased level of inflammatory cytokines, p65 and c-Jun. SGK1 was downregulated in endometritis tissues. We isolated bovine endometrial epithelial cells (bEECs) and investigated SGK1's role in inflammation by overexpressing or knocking it down, combined with transcriptome and microRNA (miRNA) sequencing in SGK1-overexpressing cells. Our results indicated that the upregulation of SGK1 reduced phospho-modification of NF-κB/JNK subunits, resulting in a reduction of IL-1β, IL-6 and TNF-α. miRNA-143 targeting transforming growth factor-β-activated kinase 1 (TAK1) was identified through mRNA and miRNA sequencing analysis, and subsequently validated in cells *via* firefly-Renilla luciferase assay. All of SGK1 expression, TAK1 knockdown, and miRNA-143 mimics significantly decreased TAK1 and inflammatory cytokines. Our results demonstrated that SGK1 inhibited the inflammatory response in the endometrium of dairy cows by targeting miRNA-143, which in turn inhibited TAK1.

To Cite This Article: Feng W, Zhou H, Umar T, Chen N, Zhang J, Liu W, Li L and Deng G, 2026. SGK1 suppresses lps-induced inflammatory responses in bovine endometrium via mir-143/tak1 axis. Pak Vet J, 46(2): 382-391. http://dx.doi.org/10.29261/pakvetj/2026.027

INTRODUCTION

Endometritis in dairy cows is one of the most important diseases affecting reproductive performance, and then resulting in reduced milk production, prolonged estrous cycles, which results in a considerable financial burden in the dairy cattle husbandry sector (Bogado *et al.,* 2023; Ren *et al.,* 2024). It is defined as a superficial inflammatory condition localized to the endometrium, sparing the deeper layers of the uterine wall. This pathology is histologically characterized by prominent infiltration of polymorphonuclear leukocytes, progressive fibrosis of the lamina propria, and marked atrophy of the uterine glands (Bogado *et al.,* 2016).

Endometritis usually occurs with bacterial infection (AbdElhafeez *et al.,* 2025). During the early stages of infection, *E. coli* plays a critical role by invading the uterine endometrial epithelial cells and releases LPS (Galvão *et al.,* 2019). The engagement of TLR4 on the cell surface by LPS initiates a signaling pathway from the plasma membrane to endosomal compartments, where the TAB2/TAK1 kinase complex orchestrates multi-site phosphorylation events (Kim *et al.,* 2023). This post-translational cascade culminates in IκBα proteasomal degradation through S32/S36 di-phosphorylation, enabling liberated NF-κB dimers (p50/p65) to translocate into the nuclear compartment for target gene transactivation (Endo *et al.,* 2025). Additionally, through p38 and JNK signaling modules, TLR stimulation propagates MAPK-dependent cellular responses (Jeong *et al.,* 2019). These mechanisms upregulate IL-1β, IL-6 and TNF-α levels within inflammatory cascades (Li *et al.,* 2023).

MiRNAs are compact non-coding RNA species operating as pivotal regulators of cellular homeostasis

through sequence-specific targeting mechanisms, thereby attenuating gene expression at the transcriptional output and mRNA translational regulatory tiers (Didiano and Hobert 2008). Numerous miRNAs have been established as regulators in the inflammatory response induced by LPS (Fu *et al.,* 2022; Kasimanickam *et al.,* 2025).

Endometrial functional integrity requires SGK1-mediated regulatory networks (Lang *et al.,* 2020). Furthermore, SGK1 mediates immune homeostasis by integrating mechanistically inflammatory signaling cascades. Dexamethasone activates SGK1 signaling in macrophages during inflammation, thereby suppressing TLR4/NF-κB activation (Liu *et al.,* 2024). In addition, SGK1 reduced the inflammatory response by promoting the transition of macrophages from M1 to M2 (Lou *et al.,* 2023). Nevertheless, the exact mechanism by which SGK1 governs the progression of endometritis remains incompletely understood.

This study investigates the regulatory mechanism of SGK1 overexpression in LPS-induced bEECs. Differentially expressed mRNAs and miRNAs were systematically identified through RNA sequencing and small RNA sequencing, followed by integrative bioinformatics analysis of the sequencing datasets. SGK1-mediated attenuation of LPS-induced inflammation was achieved through its downstream effector miRNA-143, which directly suppresses TAK1. This inhibition subsequently downregulates both NF-κB-mediated transcriptional activation and JNK-dependent phosphorylation cascades, effectively mitigating proinflammatory cytokine production. Our results reveal a novel SGK1-mediated anti-inflammatory mechanism in the pathogenesis of endometritis, which suggests its therapeutic potential through modulation of the miRNA-143/TAK1 axis. These findings identify tractable targets for the design of immunomodulatory regimens for resolution of Endometritis.

MATERIALS AND METHODS

Animals and Samples: Endometrial samples (secretions/oviduct-proximal uterine tissues) were aseptically obtained from post-slaughtered non-pregnant Holsteins during diestrus (abattoirs, Wuhan, China). Ethics approval waived by institutional guidelines as tissues were derived from abattoir samples.

Histopathological investigation: For H&E staining, endometrial tissues were fixed in 4% PFA, sectioned (5 μM), and paraffin-embedded. Histological assessment of epithelial integrity/neutrophil infiltration classified the samples into healthy (n=10) and endometritis (n=13) groups per diagnostic criteria (Bogado *et al.,* 2016).

Enzyme-Linked Immunosorbent Assay (ELISA): Uterine secretory content was analyzed for IL-6/TNF-α concentrations with manufacturer-calibrated ELISA kits (Meimian, China) following standardized protocols. Using a microplate reader (PerkinElmer, USA), we measured the absorbance at 450 nm.

Primary cell culture: Uterine specimens were collected within 30 minutes post-slaughter, transported on ice to the lab within one hour, and processed without delay. BEECs were isolated from endometrial tissues by enzymatic digestion using 1% trypsin at 4°C overnight. Following digestion, the cells were mechanically detached and washed by centrifugation at 300 × g for 5 min. Finally, the cells were cultured in DMEM/F12 medium supplemented with 20% FBS and 1% antibiotics at 37°C/5% CO_2. Prior to experimentation, cytokeratin 18 immunofluorescence confirmed cell purity (>90%).

Immunofluorescence (IF): Samples were fixed in 4% paraformaldehyde for 15 minutes, permeabilized with 0.05% Triton X-100 for 10 minutes at room temperature, and blocked with 5% BSA for 1 hour. Sequential immunostaining included overnight cold incubation with primary antibodies followed by light-protected secondary antibody treatment (1 h, RT). Nuclear counterstaining with DAPI preceded fluorescence microscopy analysis (Olympus, Japan). Table 1 provides a summary of the antibody.

Table 1: Information on antibodies used in the study

Antibodies	Catalogs	Dilution	Manufacturer
SGK1 Rabbit pAb	A1025	1:500 (WB)	ABclonal Biotechnology
Phosphp-c-Jun Rabbit pAb	AP0048	1:2000 (WB)	ABclonal Biotechnology
c-Jun Rabbit pAb	A16905	1:2000 (WB)	ABclonal Biotechnology
NF-κB p65	A2547	1:1000 (WB)	ABclonal Biotechnology
p-NF-κB p65	AP1294	1:1000 (WB)	ABclonal Biotechnolog
β-Actin Rabbit pAb	AC006	1:100000 (WB)	ABclonal Biotechnology
TAK1 Rabbit mAb	A19077	1:2000 (WB)	ABclonal Biotechnology
Phospho-TAK1 Rabbit pAb	AP0071	1:1000 (WB)	ABclonal Biotechnology
cytokeratin 18 Rabbit pAb	A1022	1:200 (IF)	ABclonal Biotechnology
HRP Goat Anti-Rabbit IgG	AS014	1:10000 (WB)	ABclonal Biotechnology
Cy3 anti-rabbit IgG	GB21303	1:100 (IF)	Servicebio

Cell viability (CCK-8) assay: bEECs (3×10^4 cells/mL) were plated in 96-well culture plates containing 100 μL medium per well and subsequently exposed to LPS (Thermo Fisher, USA) concentrations ranging from 1 to 20 μg/mL following adhesion. Viability was quantified via CCK-8 assay (10 μL/well, 12 h), with OD450 determined spectrophotometrically (PerkinElmer, USA).

Lentiviral packaging and chronic virus infection of bEECs: Lentivirus was collected 48 h post-transfection of HEK293T cells (70% confluence) co-transfected with lentiviral/packaging plasmids via Lipomaster 2000 (Vazyme, China), then used to infect bEECs, followed by puromycin (Solarbio, China) selection (1 μg/mL, 48 h). SGK1 overexpression (oS) and shRNA knockdown (shS) plasmids (GeneCreate, China) were transfected with corresponding empty vectors (pCHD-CMV-MCS-EF1-GFP-Pure and pLVX-Puro-ZsGreen1) as controls. Plasmid sequences are detailed in Table 2.

Cell Transfection: miRNA-143 mimics/inhibitors and respective NCs, along with siRNA-TAK1/NC (Gene Pharma, China) (Sequences Table 3), were transiently transfected into bEECs at 60% confluence using Lipomaster 2000 for 24h.

Table 2: The specific sequences used to downregulate and upregulate SGK1

Vectors	Sequence
pCHD-CMV-SGK1-GFP-Pure	The sequences below were inserted to the Nhe Ⅰ and Not Ⅰ sites. The sequence is underlined. GCTAGCATGACGGTGAAAACCGAGGCTGCGAGAGACACCCTCACTTACTCCAGAATGAGAGGCATGGTAGCAATT CTCATCGCTTTTATGAAACAGAGAAGGATGGGCCTGAATGACTTTATTCAGAAGATTGCCAATAACTCCTATGCATG CAAACACCCTGAAGTTCAGTCCATTTTGAAAATCTCCCCACCTCAGGAACCTGAGCTTATGAATGCCAACCCTTCTC CTCCACCAAGTCCCTCTCAGCAAATCAACCTGGGCCCATCATCCAATCCTCATGCTAAACCGTCTGACTTTCACTTC TTGAAAGTAATTGGAAAAGGCAGTTTTGGAAAGGTTCTCCTGGCAAGACACAAAGCAGAAGAAGCATTCTATGCAG TTAAAGTTTTACAAAAGAAGGCAATCCTGAAAAAGAAGGAGGAAAAGCATATTATGTCGGAGCGGAATGTTCTCCTG AAGAACGTGAAACACCCTTTCCTGGTGGGCCTTCACTTCTCTTTCCAGACGGCCGACAAACTGTACTTCGTCCTAG ACTATATTAACGGTGGAGAGTTGTTCTACCATCTCCAGAGGGAGCGATGCTTCCTGGAACCACGGGCTCGATTCTA TGCTGCTGAAATAGCCAGTGCCTTGGGTTACCTGCACTCTCTGAACATCGTTTATAGAGACTTAAAACCAGAGAATA TTTTGCTAGATTCACAAGGACACATTGTCCTTACTGACTTTGGACTCTGCAAGGAGAACATTGAACACAATGGCACA ACGTCCACCTTCTGCGGCACGCCCGAGTATCTGGCGCCTGAGGTGCTTCATAAGCAGCCCTATGATAGAACCGTG GACTGGTGGTGCCTGGGGGCCGTCTTATATGAGATGCTGTATGGCCTGCCTCCCTTTTATAGCCGAAACACAGCTG AGATGTACGACAACATTCTGAACAAGCCCCTCCAGTTGAAGCCAAATATTACAAACTCTGCAAGACATGTCCTGGAA GGCCTCCTGCAGAAGGACAGGACAAAGAGGCTGGGTGCCAAGGATGACTTTATGGAGATTAAGAATCATGTCTTCT TCTCCCTAATTAACTGGGAAGATCTCATTAATAAGAAGATTACTCCCCCTTTTAACCCAAATGTGAGCGGACCCAGC GACCTGCGACACTTTGATCCTGAGTTCACTGAAGAGCCGGTCCCCAACTCCATCGGCCGGTCCCCGGACAGCCTC CTTCTCACAGCCAGCGTCAAGGAAGCGGCTGAGGCCTTCCTGGGCTTTTCCTATGCACCTCCCATGGACTCTTTCC TCTGAGCGGCCGC
pLVX-Puro-ZsGreen1-shSGK1	The sequences below were inserted to the BamH Ⅰ and EcoR Ⅰ sites. The sequence is underlined. GGATCCGGATGGGCCTGAATGACTTTACTCGAGTAAAGTCATTCAGGCCCATCCTTTTTGAATTC

RNA extraction and RT-qPCR: Phase-separation methodology using TRIzol (Solarbio, China) yielded RNA, and cDNA generated by commercial kits (Vazyme, China). miR-143 was reverse-transcribed with stem-loop primers (Vazyme, China). qPCR analysis (Light Cycler 96, SYBR Green) (Roche, Basel, Switzerland), normalized expression to GAPDH/U6 *via* $2^{-\Delta\Delta Ct}$, primers detailed in Table 4.

Table 3: Sequences for miR and siRNA.

Gene	Sequence
mimics nc	Sense:UUCUCCGAACGUGUCACGUTT
	Anti-sense:ACGUGACACGUUCGGAGAATT
miR-143 mimics	Sense:UGAGAUGAAGCACUGUAGCUCG
	Anti-sense:AGCUACAGUGCUUCAUCUCAUU
Inhibitor nc	Sense:CAGUACUUUUGUGUAGUACAA
miR-143 inhibitor	Sense:CGAGCUACAGUGCUUCAUCUCA
siRNA-nc	Sense:UUCUCCGAACGUGUCACGUTT
	Anti-sense:ACGUGACACGUUCGGAGAATT
siRNA-TAK1	Sense:GCAGAUGAGCCGUUACAAUTT
	Anti-sense:AUUGUAACGGCUCAUCUGCTT

Table 4: qPCR Primers

Gene	sequence (5' - 3')
Bta-GAPDH	Forward: GGTCACCAGGGCTGCTTT
	Reverse: CTGTGCCGTTGAACTTGC
Bta-IL-1β	Forward: ACCGTACCTGAACCCATCAAC
	Reverse: TCCATCTCCCATGGAACCGA
Bta-IL-6	Forward: GCTTCCAATCTGGGTTC
	Reverse: GGATAATCTTTGCGTTCTTT
Bta-TNF-α	Forward: AGAGGGAAGAGCAGTCCCCAG
	Reverse: GGGCATTGGCATACGAGTCC
Bta-SGK1	Forward: AGACACCCTCACTTACTCCAGA
	Reverse: GAGGAGAAGGGTTGGCATTCA
Bta-TAK1	Forward: AGGTCATCCAGTCCTAGCGT
	Reverse: TTTGGGCATGGTGCTAGAGG
Bta-miR-143	RT:CTCAACTGGTGTCGTGGAGTCGGCAATTCAGTTGA GCGAGCTAC
	Forward: GCCGAGTGAGATGAAGCACT
	Reverse:TCAACTGGTGTCGTGGA
Bta-U6	Forward: CGAGCACAGAATCGCTTCA
	Reverse: CTCGCTTCGGCAGCACATAT

Analysis of bEECs and dairy cow tissues Protein Expression via Western Blotting: PMSF and phosphorylase inhibitors facilitated RIPA-based protein isolation (Biosharp, China). Following separation via SDS-PAGE, proteins were transferred to PVDF membranes, subjected to blocking with 5% skimmed milk (4 hours, 25°C), and incubated with primary antibodies (12 hours, 4°C) before treatment with HRP-conjugated secondary antibodies (2 hours, 25°C). The ECL substrate (Meilunbio, China) was employed to detect immunoreactive bands using Image Quant LAS 4000, quantified with ImageJ, and normalized to β-actin. Table 1 provides a summary of the antibody.

RNA and microRNA-sequencing: Total RNA (TRIzol-extracted, NanoDrop/Agilent-verified) underwent dual sequencing: RNA-seq libraries (VAHTS V10) and small RNA libraries (NEBNext) were sequenced as 150-bp paired-end reads on Illumina NovaSeq 6000 (OE Biotech, China). RNA-seq data were quality-controlled (fastp), aligned (HISAT2), and quantified (HTSeq-count); small RNA reads were adapter-trimmed/size-selected (15-41 nt). R-based differential analysis (DESeq2: DEGs $q<0.05$, $|\log_2FC|>0.85$; miRNAs $q<0.05$, $|\log_2FC|>1$) identified targets for PCA/hierarchical clustering.

Target prediction and Dual Luciferase Reporter (DLR) Assay: The psi-CHECK2-TAK1-WT and MuT vectors were synthesized by GeneCreate. The predicted binding sites for miR-143 within the TAK1-3' UTR were initially identified using the Target Scan bioinformatics tool. To experimentally validate this interaction, HEK293T cells were seeded and subsequently co-transfected for 24 hours. The transfections included either miR-143 mimics or a Negative Control (NC), paired with the appropriate reporter vector (psi-CHECK2-TAK1 WT or MuT). The dual-luciferase detection system (Yeasen, China) was subsequently used to measure luciferase activity. Measurements were taken on a Lumat LB 9507 luminometer. To account for variations in transfection efficiency, the Firefly luciferase signal was used as an internal control, and all Renilla signals were normalized against it.

Statistics Analysis: Three independent replicates' mean ± SEM is represented in the data. Statistical analysis was conducted utilizing GraphPad Prism 9.5. Statistical significance (*P<0.05; **P<0.01) was determined by two-

tailed t-tests for pairwise comparisons or Dunnett's-adjusted ANOVA for multi-group analyses.

RESULTS

SGK1 was downregulated in endometritis tissues: Histopathological analysis, using H&E staining, demonstrated that the apparent disruption of the endometrial epithelial integrity was accompanied by widespread polymorphonuclear (PMN) infiltration. Notably, signs of tissue damage, including karyopyknosis and cytolysis, were also observed. In contrast, the healthy tissues displayed a well-preserved epithelial architecture with only physiological levels of abattoir-derived tissues PMNs infiltration (Fig. 1A). Comparative analysis revealed endometrial inflammatory signature characterized by: Secretory Proteome: IL-6 and TNF-α elevation vs. controls (Fig. 1B). Transcriptional Profile: Coordinated upregulation of (*IL-6, IL-1β, TNF-α*) mRNA (Fig. 1C). The endometritis group demonstrated elevated relative phosphorylation of p65 and c-Jun (Fig. 1D). Conversely, SGK1 was significantly decreased in the endometritis group (Fig. 1E, 1F). SGK1 exhibits significantly reduced expression levels in inflammatory tissues, suggesting a potential regulatory role in the inflammatory response.

Expression levels of inflammatory factors, pathway proteins, and SGK1 in LPS-induced bEECs: The integrity of primary bEECs cells was determined through CK18 staining (Fig. 2A). After four generations of screening, the positive rate of bEECs cells exceeded 90%, indicating their suitability for subsequent experiments (Fig. 2B). bEECs were subjected to LPS (1, 5, 10 and 20μg/mL) for a duration of 60 hours. The viability of bEECs cells after 36 hours is unchanged by varying doses of LPS stimulation (Fig. 2C). In bEECs, proinflammatory cytokines exhibited a concentration-dependent relationship with LPS, but SGK1 had an inverse trend (Fig. 2D). Upon treatment of bEECs with 10μg/mL LPS for 24 hours, proinflammatory cytokine displayed an initial rapid increase followed by a gradual decline, but SGK1 exhibited an inverse trend (Fig. 2E). bEECs were exposed to LPS at different concentrations for 6 hours exhibited an increase p65/c-Jun phosphorylation in a dose-dependent manner. Concurrently, SGK1 level exhibited a marked decrease (Fig 2F, 2G). Furthermore, in bEECs exposed to 10μg/mL LPS for 24 hours, signaling (p65/c-Jun phosphorylation) exhibited a gradual rise, with significant differences observed after 6 hours. In contrast, SGK1 exhibited a progressive decline during the same experiments (Fig. 2H, 2I). The following tests were conducted under the conditions of bEECs stimulated with 10μg/mL LPS for 6 hours.

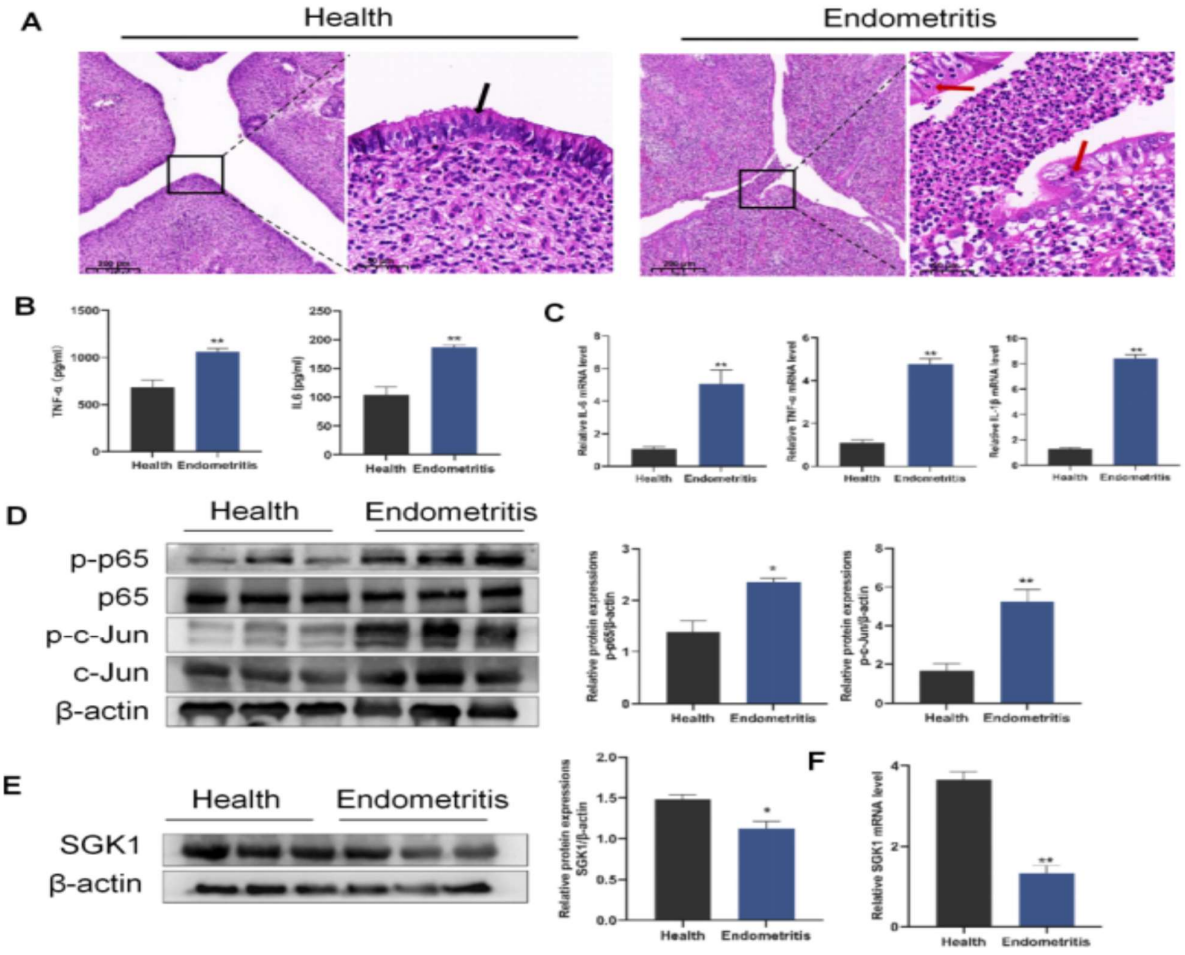

Fig. 1: The expression levels of SGK1, cytokines, and key proteins are associated with inflammatory signaling pathways in endometrial tissue. (A) H&E-stained images of endometrial tissue. 100×magnificention, 400×magnificention; Red arrow: PMN; Black arrow: bEECs. (B) ELISA confirmed IL-6/TNF-α in endometrial secretions from the healthy and endometritis groups. (C) RT-qPCR analysis measured cytokine transcripts (*IL-6/IL-1β/TNF-α*). (D) WB was employed to assess p65/c-Jun phosphorylation. (E) WB was utilized to analyze the levels of SGK1. (F) RT-qPCR analysis measured *SGK1*. *P<0.05, ** P<0.01.

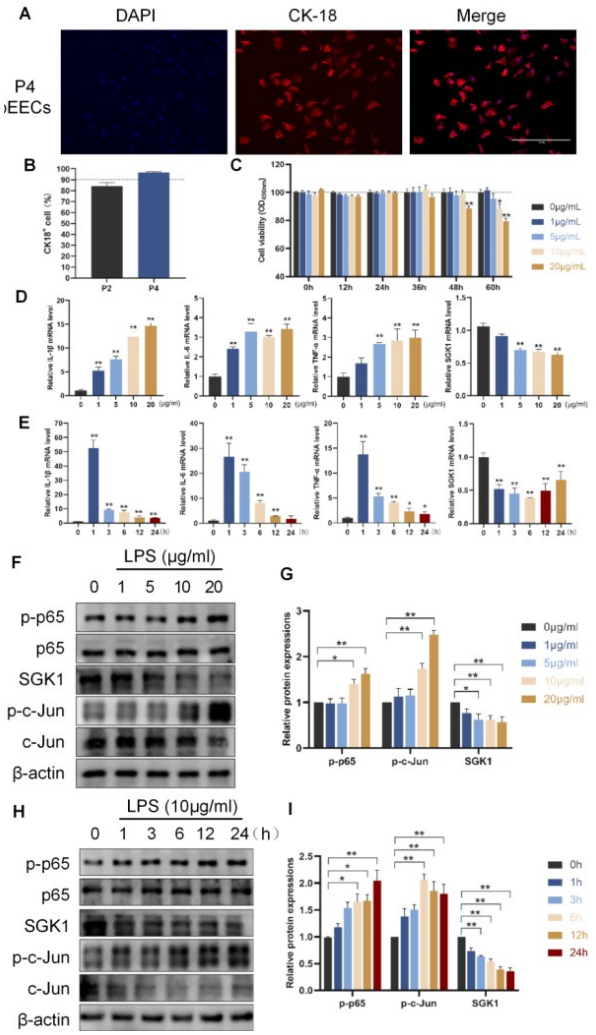

Fig. 2: LPS modulates the levels of SGK1, cytokines, and key proteins associated with the inflammatory signaling pathway. (A) The cell membranes were stained with an epithelial cell-specific marker cytokeratin 18, and nuclei were labeled by DAPI. Scale bars: 200μM. (B) P4 bEECs CK-18-positive cell percentage was determined by immunofluorescence. (C) CCK-8 assay quantified viable cell proportions. Incubation of cells with graded LPS doses (0, 1, 5, 10 and 20 μg/mL) at various durations (12, 24, 36, 48, and 60 h) was performed. (D) RT-qPCR analysis measured cytokine and *SGK1* transcripts. bEECs treated with varying LPS doses (0-20 μg/mL) during a 6-hour incubation period were assessed using RT-qPCR. (E) RT-qPCR analysis measured cytokine and *SGK1* transcripts. bEECs treated with 10 μg/mL LPS across defined timepoints (0-24 h sampling at 1,3,6,12,24 h marks). (F, G) WB was utilized to analyze p65/c-Jun phosphorylation and SGK1 in bEECs stimulated with graded LPS dose levels (0-20 μg/mL) during a 6-hour incubation period. (H, I) WB was utilized to analyze p65/c-Jun phosphorylation and SGK1 in bEECs stimulated with 10 μg/mL LPS across defined timepoints (0-24 h sampling at 1,3,6,12,24 h marks). *P<0.05, **P<0.01.

Overexpression of SGK1 in bEECs suppresses LPS-induced inflammatory: To delineate SGK1-mediated signaling in LPS-challenged bEECs. We successfully established lentivirus-mediated bEECs with SGK1 overexpression. The oS group exhibited significant upregulation in both mRNA transcription and protein expression levels of SGK1 (Fig. 3A, 3B). SGK1 overexpression suppressed LPS-induced pro-inflammatory signaling, attenuating cytokines production (Fig. 3C) while inhibiting phosphorylation of p65 and c-Jun (Fig. 3D, 3E). The results verified that elevated SGK1 expression reduces LPS-induced inflammatory responses in cells.

SGK1 knockdown in bEECs does not affect LPS-induced inflammation: In bEECs, lentivirus-mediated SGK1 silencing was confirmed via qPCR and immunoblotting (Fig. 4A, 4B). LPS comparably induced both transcriptional (*IL-6*, *IL-1β*, *TNF-α*) and signaling (p65/c-Jun phosphorylation) inflammatory responses in shS and control groups (Fig. 4C-4E).

Silencing TAK1 inhibited LPS-induced cellular inflammatory responses: Transcriptome analysis revealed significant downregulation of TAK1 expression in SGK1-overexpressing cells compared to controls (log_2FC = -0.99, q<0.05) (Table S1). SGK1 overexpression significantly suppressed TAK1 mRNA levels in bEECs (Fig. 5A). LPS treatment enhanced TAK1 phosphorylation, without affecting total protein levels in the negative control group, whereas SGK1 overexpression led to concomitant downregulation of both total TAK1 expression and its phosphorylation status (Fig. 5B). To explore the role of TAK1 in cellular inflammatory responses, bEECs were transfected with siRNA-TAK1 (siRNA-TAK1 group) and siRNA negative control (siRNA-nc group) and then stimulated with LPS. TAK1 silencing suppressed LPS-driven inflammation in bEECs, attenuating cytokine (*IL-6*, *IL-1β,* and *TNF-α*) production while abolishing TAK1 phosphorylation cascades and downstream effectors p65/c-Jun (Fig. 5C-5E). In addition, TAK1 silencing suppressed LPS-induced nuclear import of p65/c-Jun in bovine endometrial epithelia (Fig. 5F, 5G). These findings collectively established TAK1 as a master regulatory hub for both NF-κB and JNK signaling axes in bEECs.

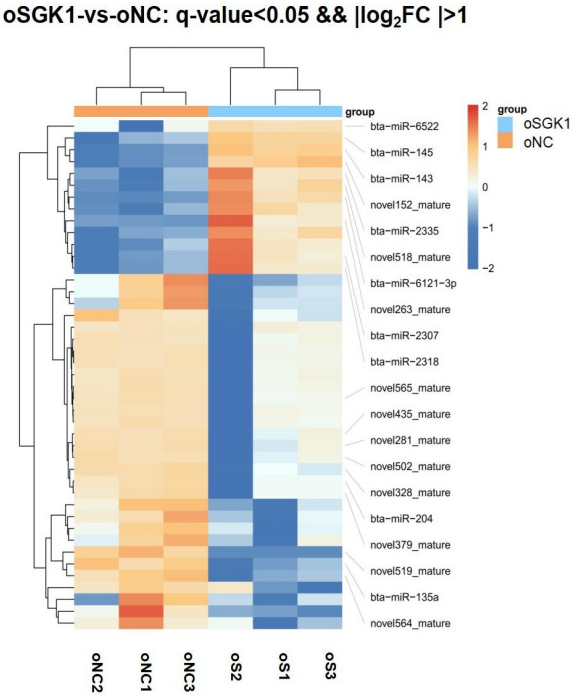

Fig. S1: Differential expression of miRNA.

SGK1 increases miRNA-143 targeting TAK1: The differentially expressed miRNAs are shown in Supplementary Data Figure 1. SGK1 overexpression upregulated miR-143 expression in bEECs (Fig. 6A).

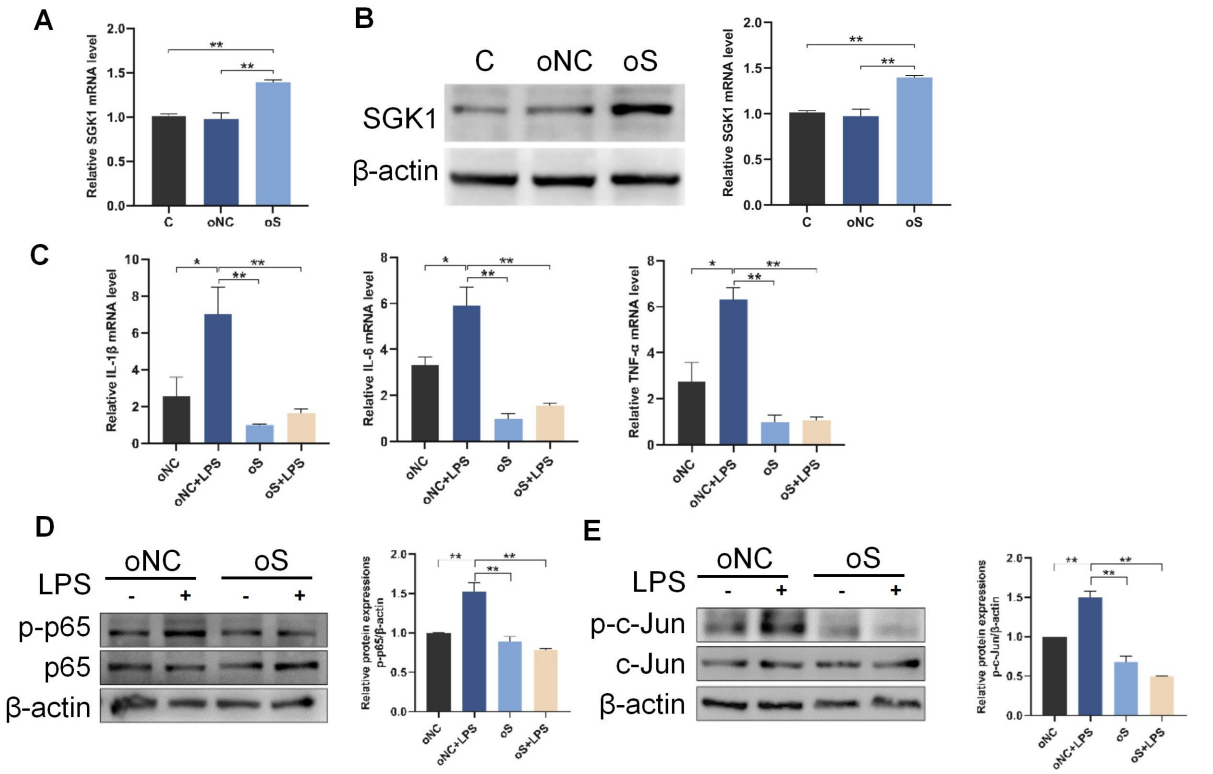

Fig. 3: SGK1 overexpression in bEECs. (A) RT-qPCR analysis measured *SGK1* transcripts in C, oNC and oS group. (B) WB was utilized to analyze the levels of SGK1 in C, oNC and oS group. (C) oNC and oS group were incubated with or without LPS. RT-qPCR analysis measured cytokine transcripts. (D, E) oNC and oS group were incubated with or without LPS. WB was utilized to analyze p65/c-Jun phosphorylation. C: control, oNC: bEECs with negative control, oS: bEECs with overexpression of SGK1. *P<0.05, **P<0.01.

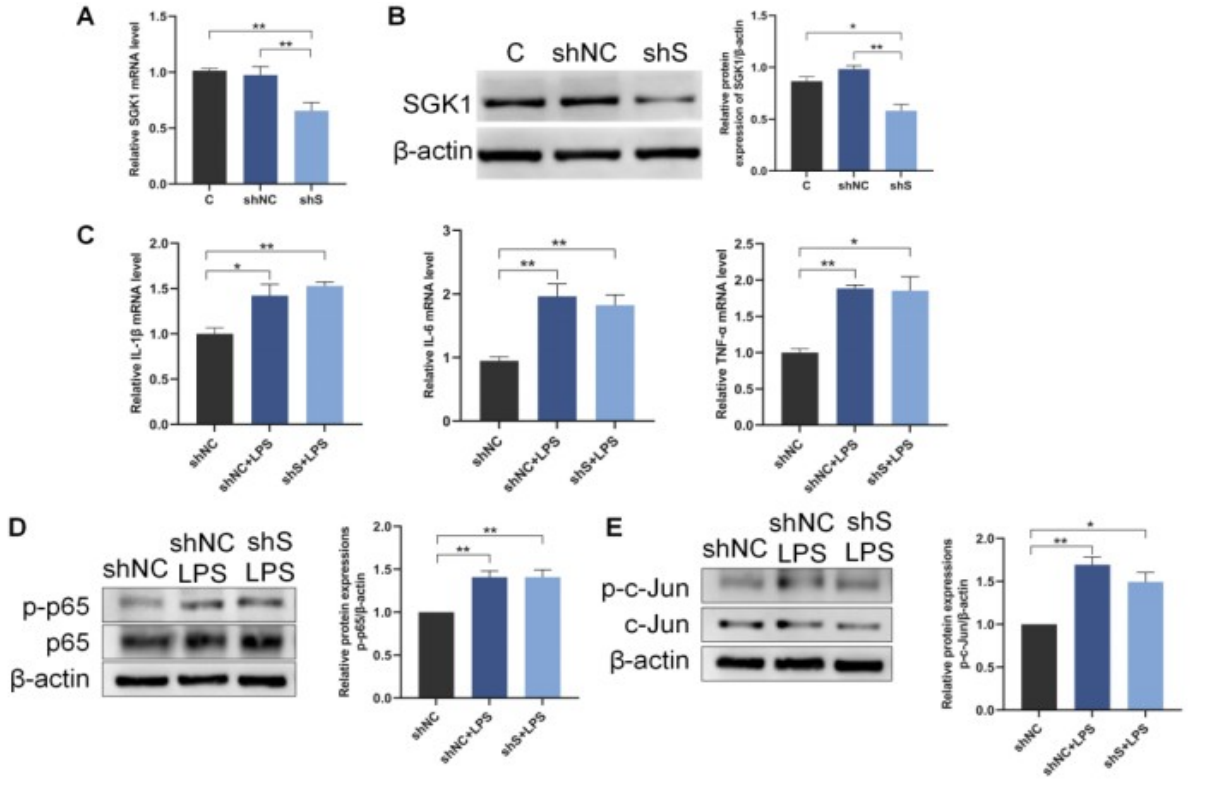

Fig. 4: SGK1 Knockdown on bEECs. (A) RT-qPCR analysis measured *SGK1* transcripts in the C, shNC, and shS groups. (B) WB was utilized to analyze the levels of SGK1 in C, shNC and shS group. (C) The shNC and shS groups were incubated with or without LPS. RT-qPCR analysis measured cytokine transcripts. (D, E) The shNC and shS groups were incubated with or without LPS. WB was employed to assess p65/c-Jun phosphorylation. C represents the control group, shNC denotes bEECs treated with shRNA negative control, and shS indicates bEECs with SGK1 knockdown. *P<0.05, **P<0.01.

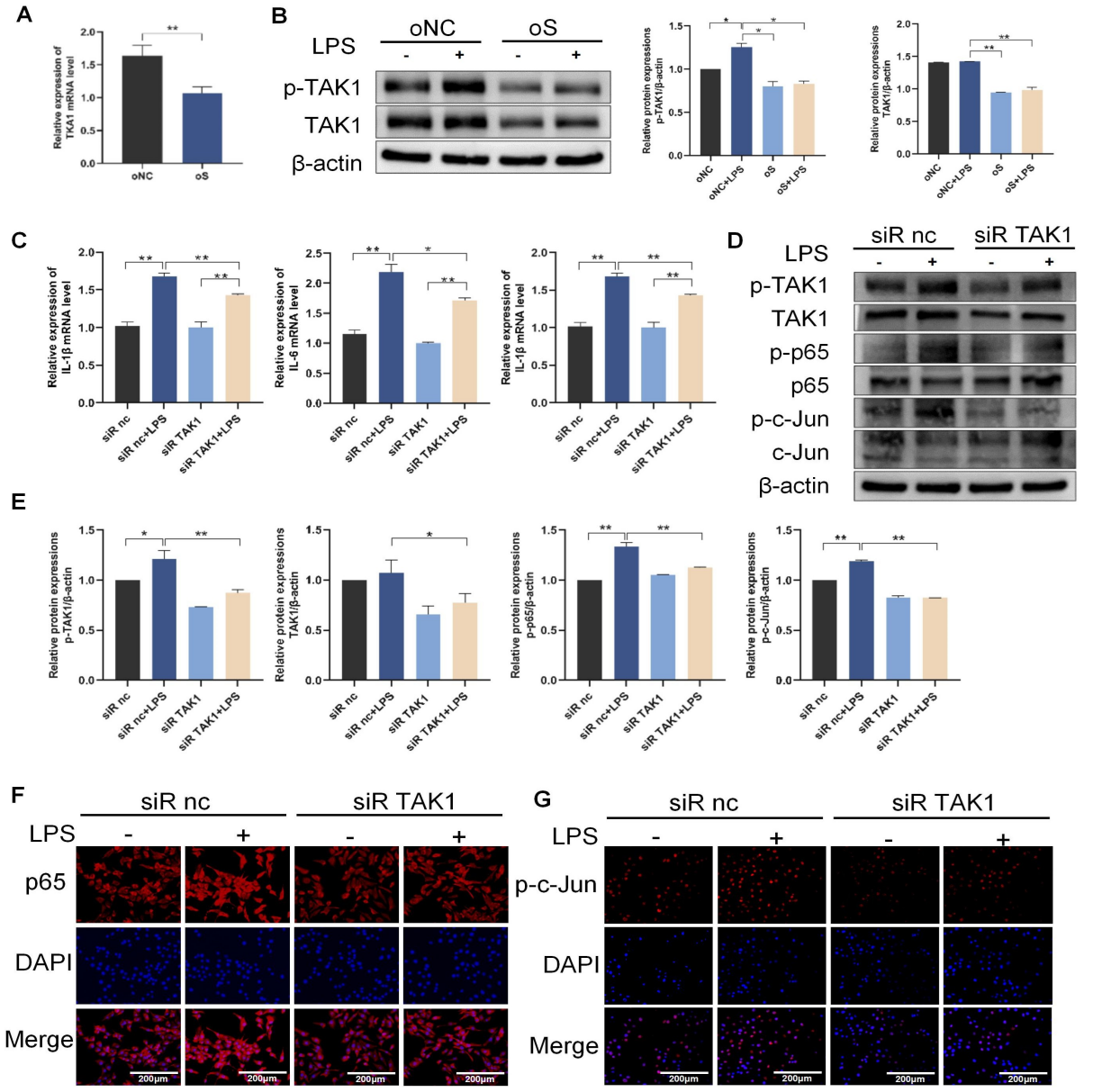

Fig. 5: TAK1 inhibition suppressed LPS-induced inflammation. (A) The TAK1 expression level was evaluated with RT-qPCR in bEECs exhibiting SGK1 overexpression. (B) The oNC and oS groups were incubated with or without LPS. WB was utilized to analyze the concentrations of p-TAK1 and TAK1. (C) RT-qPCR analysis measured cytokine transcripts. (D, E) WB was employed to examine the protein concentrations of p-TAK1, TAK1, p-p65, and p-c-Jun. (F, G) Nuclear translocation of p65 and p-c-Jun was evaluated using immunofluorescence. Scale bar: 200 μM. siR nc: siRNA nc was transfected into bEECs and treated for 24 hours; siR TAK1: siRNA-TAK1 was transfected into bEECs and incubated for 24 hours; siR nc+LPS and siR TAK1+LPS: bEECs were incubated with LPS. *P<0.05, **P<0.01.

Subsequently, Transfection with miR-143 mimics significantly downregulated TAK1 in bEECs (Fig. 6B, 6C). Meanwhile, administration of a miR-143 inhibitor in SGK1-overexpressing cells substantially restored TAK1 mRNA and protein levels (Fig. 6D, 6E). The binding sites were predicted as AGUAGAGU of miRNA-143 to the 3' UTR region of TAK1 through Target Scan and constructed Wt TAK1 and Mut TAK1 plasmids (Fig. 6G). When the plasmids and mimics were co-transfected into 293T cells, the DLR assays confirmed that the transfection of miRNA-143 mimics could effectively reduce the luciferase activity of the Wt-TAK1 3' UTR plasmid whereas showed no effect on Mut-TAK1 (Fig. 6F). In conclusion, this test suggests that SGK1 inhibits TAK1 expression through miRNA-143.

miR-143 attenuates LPS-stimulated inflammation: Primarily to examine the function of miR-143 in LPS-triggered inflammatory responses, bEECs were transfected with miR mimics over a 24-hour period. Subsequently, cells were stimulated with or without LPS. In bEECs, miR-143 mimics attenuated LPS-induced pro-inflammatory responses, suppressing both cytokine expression and phosphorylation of p65/c-Jun via direct targeting of TAK1 (Fig. 7A, 7B). Meanwhile, IF staining demonstrated impaired nuclear import of both p65 and c-Jun following miR-143 overexpression (Fig. 7C, 7D). Collectively, these findings demonstrated that miR-143 attenuates inflammation by directly targeting TAK1.

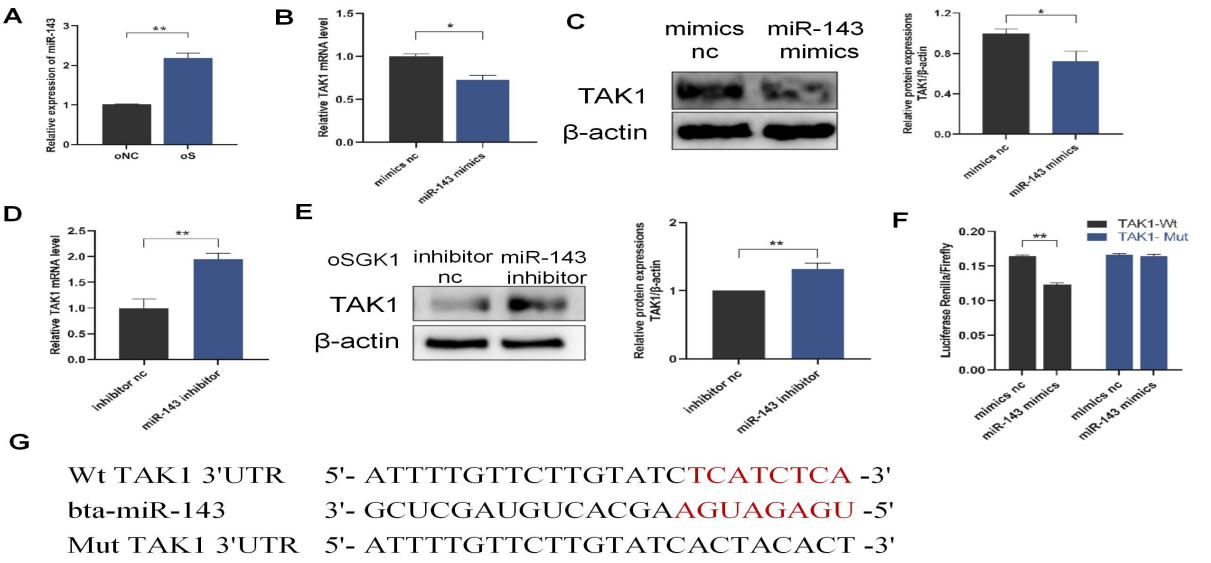

Fig. 6: The SGK1 targets TAK1 through miRNA-143. (A) The expression level of miRNA-143 was evaluated *via* RT-qPCR in bEECs exhibiting SGK1 overexpression. (B, C) miR-143 mimics and nc were transfected into bEECs for 24h. RT-qPCR analysis measured *TAK1* transcripts. WB was employed to assess the levels of TAK1. (D, E) The miRNA-143 inhibitor and negative control were transfected into bEECs with SGK1 overexpression for 24 hours. Western blotting was employed to assess the levels of TAK1. RT-qPCR analysis measured *TAK1* transcripts. WB was employed to assess the levels of TAK1. (F) The Wt/Mut-TAK1 3′UTR was co-transfected with mimics into HEK293T cells, subsequently measuring luciferase activity. (G) Proposed binding motif of bta-miR-143 situated inside the TAK1 3′UTR region. mimics nc: bEECs with miRNA mimics nc, miR-143 mimics: bEECs exhibiting overexpression of miRNA-143. oNC: bEECs with negative control; oS: bEECs with SGK1 overexpression. mimics nc: bEECs with miRNA mimics nc, miR-143 mimics: bEECs exhibiting overexpression of miRNA-143. *P<0.05, **P<0.01.

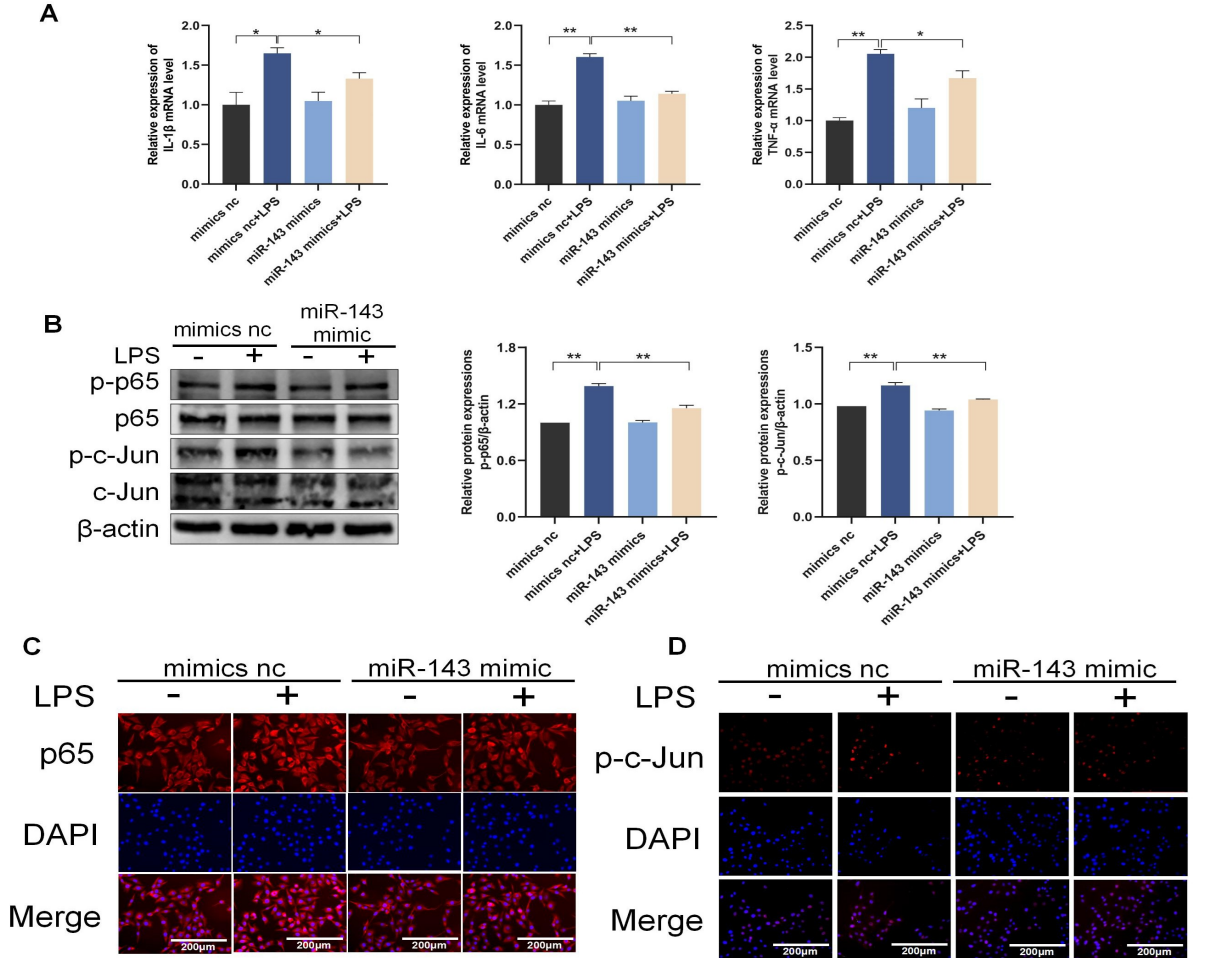

Fig. 7: miR-143-transfected bEECs. Mimics nc and miR-143 mimics were transfected into bEECs and cultured for 24 h. Then bEECs were stimulated with or without LPS. (A) RT-qPCR analysis measured cytokine transcripts. (B) WB was employed to assess p65/c-Jun phosphorylation. (C, D) IF visualized nuclear trafficking of p65/phospho-c-Jun. Scale bars: 200μm. *P<0.05, **P<0.01.

DISCUSSION

The endometrial epithelium, functioning as the cow's first line of defense, orchestrates innate immune responses (Tinning *et al.,* 2023). BEECs utilize pathogen recognition receptors to identify microbial-associated molecular patterns from infectious agents, triggering signal transduction pathways that induce inflammatory mediator secretion upon receptor activation (Aflatoonian *et al.,* 2007; Vaidhya *et al.,* 2025). This coordinated immune response facilitates pathogen clearance by recruiting neutrophils and macrophages to the infection site. However, persistent or excessive activation of these pathways induces pathological inflammation and irreversible endometrial damage. This dual functionality underscores the delicate balance between protective immunity and tissue homeostasis, with implications for bovine reproductive health and fertility outcomes.

SGK1 has emerged as a pivotal regulatory node in innate immunity and a promising therapeutic target. A previous study demonstrated an inverse correlation between SGK1 expression and LPS concentration (Chen *et al.,* 2024), a pattern consistent with our observations. Additionally, DEX and insulin have been shown to upregulate SGK1 transcription and translation, thereby suppressing LPS-induced cytokine production by blocking NF-κB and JNK (Zhu *et al.,* 2012; Mansley *et al.,* 2016). However, these findings have been exclusively derived from murine models and human cell lines. Notably, this study provides the first evidence in primary bovine endometrial epithelial cells that lentiviral vector-mediated stable SGK1 overexpression significantly attenuates LPS-induced phosphorylation of p65 and c-Jun. Subsequently, we demonstrated that SGK1-mediated suppression of these phospho-signaling intermediates functionally links SGK1 activity to the inhibition of two canonical inflammatory cascades.

Emerging evidence indicates that the SGK1-TAK1 axis is a critical modulator of inflammatory signaling. Previous studies revealed that siRNA-mediated SGK1 knockdown in macrophages exacerbates LPS-induced NF-κB nuclear translocation and inflammatory responses, potentially through enhanced TAK1 phosphorylation (Zhou *et al.,* 2015). Complementary work in porcine epidemic diarrhea virus-infected Vero cells demonstrated that TAK1 drives JNK/c-Jun activation via MKK4 phosphorylation, whereas TAK1 silencing attenuates both its phosphorylation and downstream JNK signaling (Wang *et al.,* 2022). These findings align with reports that LPS stimulates TAK1 autophosphorylation to activate NF-κB and JNK pathways, then initiates inflammatory and apoptotic cascades (Sun *et al.,* 2024; Liu *et al.,* 2025). Moreover, our investigation reveals two mechanistically convergent observations: Transcriptomic profiling and immunoblotting of SGK1-overexpressing cells demonstrated significant downregulation of TAK1 mRNA and total protein levels; TAK1 knockdown via siRNA replicated SGK1 overexpression's anti-inflammatory effects, reducing LPS-triggered cytokine production. These parallel outcomes establish TAK1 suppression as a mechanism by which SGK1 governs inflammatory homeostasis.

MicroRNAs (miRNAs) represent master regulators of biological processes, fine-tuning epithelial functionality and immune cell differentiation while critically governing inflammatory responses (Chen *et al.,* 2018; Fu *et al.,* 2022). SGK1 has been shown to phosphorylate the transcription factor Specificity Protein-1 (SP1), thereby enhancing its transcriptional activity and upregulating nuclear transport regulators (RANBP1, RANGAP1, RANGTP) and subsequently modulating XPO5/Ran-GTP-dependent pre-miRNA nuclear export and maturation (Amato *et al.,* 2013; Dattilo *et al.,* 2017). Building upon this, we proposed that SGK1-mediated TAK1 suppression operates through miRNA reprogramming. Comparative analysis of miRNA sequencing data with bioinformatic prediction tools revealed TAK1 as a putative miR-143 target gene, which was subsequently confirmed through dual-luciferase reporter assays. This regulatory interaction aligns with prior studies (Huang *et al.,* 2017; Xu *et al.,* 2025). An integrative analysis of miRNA sequencing independent RT-qPCR validation demonstrated that SGK1 overexpression induced miR-143 expression. miR-143 mimic transfection phenocopied SGK1's anti-inflammatory actions, manifesting as reduced TAK1 protein abundance, attenuated LPS-induced cytokine secretion, and suppressed nuclear translocation (p65/c-Jun). These findings are consistent with the mechanism by which miR-143 can improve autoimmune hepatitis by targeting the expression of TAK1 in mouse liver cells (Tu *et al.,* 2020).

In summary, SGK1 was expressed lowly in endometritis tissues of dairy cows. However, high expression of SGK1 significantly suppressed the inflammatory response by promoting miRNA-143–mediated targeting of TAK1, thereby inhibiting NF-κB (p65) and JNK (c-Jun) signaling, and further inhibited the inflammatory response within uterine compartments. This finding partially illustrates the regulatory mechanism of SGK1 on the development of endometritis in dairy cows.

Authors contribution: Study design and conceptualization were carried out by WF and GZD. WF, HZ, and TU carried out animal preparation and performed experiments and data analysis. CNE, JXZ, LYL, and WJL participated in some experiments. Figures were produced by WF and HZ. The initial version of the manuscript was drafted by WF, with subsequent revisions and final endorsement provided by all contributing authors.

Data availability: Contact corresponding author for access requests.

Funding: This work was funded through NSFC funding (Grant No. 31972744).

Institutional review board statement: Not applicable.

Acknowledgments: We express our gratitude to laboratory members and slaughterhouse workers who provided advice and support for this study. The constructive comments from the reviewers and editors are acknowledged.

Competing interest: There are no conflicts of interest to report.

REFERENCES

AbdElhafeez NE, El-Darier SM, Gryazneva TN, *et al.*, 2025. Assessment of the antimicrobial efficacy of probiotics, biosynthesized silver nanoparticles, and their combination with physical irradiations against cattle endometritis pathogens. Scientific Reports 15(1): 32572.

Aflatoonian R, Tuckerman E, Elliott SL, *et al.*, 2007. Menstrual cycle-dependent changes of Toll-like receptors in endometrium. Human Reproduction 22(2): 586–593.

Amato R, Scumaci D, D'Antona L, *et al.*, 2013. Sgk1 enhances RANBP1 transcript levels and decreases taxol sensitivity in RKO colon carcinoma cells. Oncogene 32(38): 4572–4578.

Bogado PO, Hostens M, Dini P, *et al.*, 2016. Comparison between cytology and histopathology to evaluate subclinical endometritis in dairy cows. Theriogenology 86(6): 1550–1556.

Bogado PO, LeBlanc SJ, Gnemi G, *et al.*, 2023. Genesis of clinical and subclinical endometritis in dairy cows. Reproduction 166(2): R15–R24.

Chen D, Li K, Pan L, *et al.*, 2024. MicroRNA-223-3p Targeting SGK1 Regulates Apoptosis and Inflammation in Sepsis-Associated Acute Kidney Injury. Kidney & Blood Pressure Research 49(1): 657–666.

Chen Q, Wu S, Wu Y, *et al.*, 2018. MiR-149 suppresses the inflammatory response of chondrocytes in osteoarthritis by down-regulating the activation of TAK1/NF-κB. Biomedicine & Pharmacotherapy 101: 763–768.

Dattilo V, D'Antona L, Talarico C, *et al.*, 2017. SGK1 affects RAN/RANBP1/RANGAP1 via SP1 to play a critical role in pre-miRNA nuclear export: a new route of epigenomic regulation. Scientific Reports 7: 45361.

Didiano D and Hobert O, 2008. Molecular architecture of a miRNA-regulated 3' UTR. RNA 14(7): 1297–1317.

Endo A, Takahashi C, Ishibashi N, *et al.*, 2025. Ubiquitination-activated TAB-TAK1-IKK-NF-κB axis modulates gene expression for cell survival in the lysosomal damage response. eLife 14: RP106901.

Fu Q, Yu W, Fu S, *et al.*, 2022. MicroRNA-449c-5p alleviates lipopolysaccharide-induced HUVECs injury via inhibiting the activation NF-κb signaling pathway by TAK1. Molecular Immunology 146: 18–26.

Galvão KN, Bicalho RC and Jeon SJ, 2019. Symposium review: The uterine microbiome associated with the development of uterine disease in dairy cows. Journal of Dairy Science 102(12): 11786–11797.

Huang FT, Peng JF, Cheng WJ, *et al.*, 2017. MiR-143 Targeting TAK1 Attenuates Pancreatic Ductal Adenocarcinoma Progression via MAPK and NF-κB Pathway In Vitro. Digestive Diseases and Sciences 62(4): 944–957.

Jeong MH, Park YJ, Kim HR, *et al.*, 2019. Polyhexamethylene guanidine phosphate-induced upregulation of MUC5AC via activation of the TLR-p38 MAPK and JNK axis. Chemico-Biological Interactions 305: 119–126.

Kasimanickam R, Bhowmik P, Kastelic J, *et al.*, 2025. From infection to infertility: Diagnostic, therapeutic, and molecular perspectives on postpartum metritis and endometritis in dairy cows. Animals 15(19): 2841.

Kim HJ, Kim H, Lee JH, *et al.*, 2023. Toll-like receptor 4 (TLR4): new insight immune and aging. Immunity & Ageing 20(1): 67

Lang F, Rajaxavier J, Singh Y, *et al.*, 2020. The Enigmatic Role of Serum & Glucocorticoid Inducible Kinase 1 in the Endometrium. Frontiers in Cell and Developmental Biology 8: 556543.

Li Z, Pan H, Yang J, *et al.*, 2023. Xuanfei Baidu formula alleviates impaired mitochondrial dynamics and activated NLRP3 inflammasome by repressing NF-κB and MAPK pathways in LPS-induced ALI and inflammation models. Phytomedicine 108: 154545.

Liu H, Zhou L, Wang X, *et al.*, 2024. Dexamethasone upregulates macrophage PIEZO1 via SGK1, suppressing inflammation and increasing ROS and apoptosis. Biochemical Pharmacology 222: 116050.

Liu Y, Zhai Y, Ma L, *et al.*, 2025. Colchicine alleviates ischemic white matter lesions and cognitive deficits by inhibiting microglia inflammation via the TAK1/MAPK/NF-κB signaling pathway. Behavioural Brain Research 490: 115619.

Lou Y, Fu Z, Tian Y, *et al.*, 2023. Estrogen-sensitive activation of SGK1 induces M2 macrophages with anti-inflammatory properties and a Th2 response at the maternal-fetal interface. Reproductive Biology and Endocrinology 21(1): 50.

Mansley MK, Watt GB, Francis SL, *et al.*, 2016. Dexamethasone and insulin activate serum and glucocorticoid-inducible kinase 1 (SGK1) via different molecular mechanisms in cortical collecting duct cells. Physiological Reports 4(10).

Ren X, Lu H, Wang Y *et al.*, 2024. Phenotypic and genetic analyses of mastitis, endometritis, and ketosis on milk production and reproduction traits in Chinese Holstein Cattle. Animals 14(16): e12792.

Sun T, Wang F, Li J, *et al.*, 2024. ISIR and its human homolog gene AK131315 strengthen LPS-induced inflammation and acute lung injury by promoting TAK1-dependent NF-κB and MAPK signaling. International Immunopharmacology 137: 112510.

Tinning H, Edge JC, DeBem THC, *et al.*, 2023. Review: Endometrial function in pregnancy establishment in cattle. Animal 17 Suppl 1: 100751.

Tu H, Chen D, Cai C, *et al.*, 2020. microRNA-143-3p attenuated development of hepatic fibrosis in autoimmune hepatitis through regulation of TAK1 phosphorylation. Journal of Cellular and Molecular Medicine 24(2): 1256–1267.

Vaidhya A, Ravi PG, Deepthi V, *et al.*, 2025. RLR pathways in pregnancy: Guardians of antiviral immunity and mediators of inflammation-driven complications. Journal of Reproductive Immunology 172: 104637.

Wang J, Kan X, Li X, *et al.*, 2022. Porcine epidemic diarrhoea virus (PEDV) infection activates AMPK and JNK through TAK1 to induce autophagy and enhance virus replication. Virulence 13(1): 1697–1712.

Xu Y, Song Y, Zhang C, *et al.*, 2025. Mesenchymal stem cells-derived miR-143-3p attenuate acute kidney injury by suppressing TAK1-Driven necroptosis. Biochemical and Biophysical Research Communications 778: 152339.

Zhou H, Gao S, Duan X, *et al.*, 2015. Inhibition of serum- and glucocorticoid-inducible kinase 1 enhances TLR-mediated inflammation and promotes endotoxin-driven organ failure. FASEB Journal 29(9): 3737–3749.

Zhu T, Zhang W and Wang DX, 2012. Insulin up-regulates epithelial sodium channel in LPS-induced acute lung injury model in rats by SGK1 activation. Injury 43(8): 1277–1283.